Determination of the Orientation of an Object within a 3D Space. Implementation and Example Applications

Krzysztof Różanowski, Jarosław Lewandowski, and Marek Placha

***Abstract*—The article presents a design of a measurement system implementing algorithms for determination of the orientation of objects within three-dimensional space using am integrated triaxial MEMS system, magnetometer, and Madgwick's AHRS sensor fusion algorithm. Also included in the proposed implementation are the algorithms for calibration of sensors.**

Estimated orientation of the object of interest is provided using Euler's angles or quaternions The system consists of a data acquisition system and software to visualize the acquired data. The main components of the acquisition system include a microcontroller featuring ARM Cortex M4 processor core and integrated 9DOF module consisting of an accelerometer, gyroscope, and magnetometer.

The measurement system is capable of communicating with other devices via a Bluetooth interface. The measurements of the monitored values read by 9DOF sensors may be collected at sampling frequencies of up to 100Hz. Options to save data to SD cards and to maintain power supply from a battery are also available.

The proposed solution is characterized by low construction costs, small dimensions, and ease of implementation in all types of systems. It can be used for example in mapping the movement of limbs (spatial orientation of the foot, detection of gait cycle phases, assessment of motor activity), as a support tool in inertial navigation systems or in the control of objects in motion (aerial vessels, mechanical vehicles). The article also presents an application of the system as a limb motion capture device.

***Index Terms*—AHRS, biomedical electronics, IMU, motion capture, spatial orientation.**

I. Introduction

THE possibility of real-time determination of the orientation of objects within a three-dimensional space may be useful in multiple system applications. Possible embodiments of location identification systems may include systems of cameras and markers placed on the monitored object, connection of encoders or inertial sensors being placed on the moving object. The article presents an embodiment that makes use of inertial sensors being part of the MEMS (Micro-Electro-Mechanical Systems) technology. The MEMS technology facilitates significant miniaturization of system and reduction of sensor construction costs. Sensors of this type are readily available at the market [4]. An inertial measurement unit (IMU) was developed on the basis of these sensors and completed with a magnetometer to form a MARG (Magnetic, Angular Rate, and Gravity) sensor system.

Many types of sensor fusion algorithms are used for the processing of data acquired from the gyroscope, accelerometer, and magnetometer [6]. The presented solution features Madgwick's AHRS algorithm, that estimates spatial orientation using quaternion values. Euler's angles are another method for representing rotation, also provided by the proposed system.

Thanks to their small overall dimensions, MARG systems may be used for determination of spatial orientation of moving objects, e.g. multirotor vessels [2][3], humanoid robots (multiple degrees of freedom required) [5], mechanical vehicles [12][13], as well as for the capture of limb motion and subsequent analysis of motor activity of subjects [11].

The study was co-financed by the National Centre for Research and Development as part of the project no. DOBR/0038/R/ID2/2013/03 titled "A microsensor technology for the measurement of vital functions in soldiers – an element of the personal monitoring system".

II. System Layout

The system is comprised of two main elements: an acquisition system and a desktop script for the visualization of data. An important assumption for the presented solution consisted in its small dimensions ensuring versatility of applications. The main component of the acquisition system consists of a microcontroller that collects data from measurement sensors, applies a special algorithm to determine the spatial orientation of the object, saves data to an SD card and communicates with external systems via a Bluetooth interface. A block diagram of the system is presented in Fig. 1.

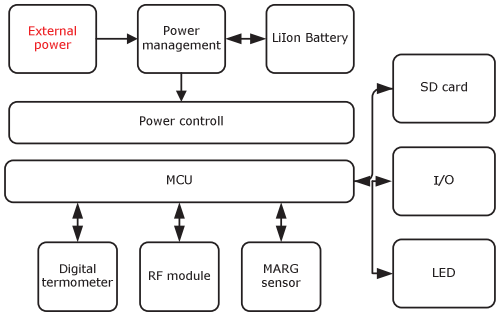

Fig. 1. Block diagram of the measurement device.

K. Różanowski, J. Lewandowski and M. Placha are with Military Institute of Aviation Medicine, Krasińskiego 54/56, 01-755 Warsaw, Poland (e-mail: krozan@wiml.waw.pl).

The microcontroller features a 32-bit ARM Cortex M4 processor core model STM32F405RG. The high CPU rate (168 MHz) and relatively high memory (192 kB RAM) of the processor, as well as the presence of an FPU coprocessor capable of hardware processing of floating point variables allow for implementation of the orientation determination algorithms used in the system as well as for future enhancement of system's capabilities The acquisition module features a MARG (magnetic, angular rate, and gravity) sensor system. An LSM9DS0 integrated circuit from ST Microelectronics has been used, integrating a triaxial accelerometer, a gyroscope, and a magnetometer to provide 9 degrees of freedom (9DOF). MARG measures the acceleration, angular velocity, and magnetic field induction with sampling frequency of up to 100 Hz. The solution is inexpensive and easy to operate; it also allows to significantly reduce the number of electronic elements within the system. A radio interface is dedicated to communicate with external devices (PC with desktop script). The wireless interface conforming to the Bluetooth 2.1 standard is based on an RN-41 module. The system is supplied from external power source and features battery power maintenance. Power management is achieved by means of a BQ24072 integrated system. The layout of the acquisition system is presented in Fig. 2.

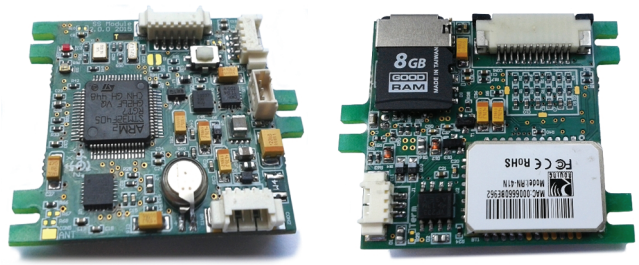

Fig. 2. Data acquisition module.

All electronic components are manufactured using SMT technology. Module dimensions are 35 mm/35 mm. The system is powered in the voltage range of 5 V-12 V .

III. ALGORITHMS

A. *Representation of orientation*

The system delivers the determined orientation as a normalized quaternion or using Euler's angles.

The quaternion is an algebraic structure involving an extension of the field of complex numbers [1][8]. The algebraic form of the quaternion is as follows (1):

$$q = w + xi + yj + zk \tag{1}$$

The w component of quaternion q is referred to as the real component while the x, y, z components are imaginary components. The quaternion may be interpreted as a vector within an R(3) space and an angle of rotation around that vector. In this interpretation, w is the scalar part, and x, y, z are the vector part of the quaternion [3]. An advantage of quaternion representation consists in quick combination of rotations (multiplication of quaternions), quick inversion of rotations, and quick conversion between representations of rotations (rotation matrices/Euler's angles) [9], avoid a phenomenon called gimbal lock.

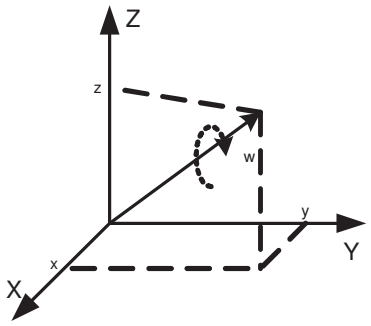

Fig. 3. Interpretation of the quaternion [3].

Euler's angles are a system of three angles that facilitate unambiguous determination of an object within Euclidean space [1]. One of the nomenclatures used for this group of angles includes the terms such as yaw (rotation along the Z axis), pitch (rotation along the Y axis), and roll (rotation along the X axis) [16]. This representation is illustrated in Fig. 4.

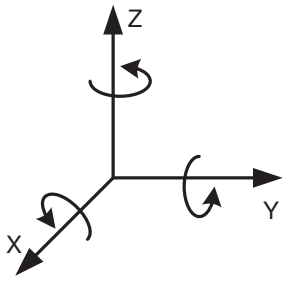

Fig. 4. Illustration of Euler's angles.

An advantage of Euler's angles consists in their intuitiveness; however, in case of particular rotations, a peculiarity may be encountered consisting in a loss of a degree of freedom.

B. *Accelerometer calibration*

In order to obtain correct results from the inertial sensors and the magnetometer, they should be subjected to calibration before the measurements. Unprocessed data may be burdened by a significant error. Calibration of the accelerometer is carried out using the following equation [15](2):

$$\begin{bmatrix} A_{x1} \\ A_{Y1} \\ A_{Z1} \end{bmatrix} = \begin{bmatrix} ACC_{11} & ACC_{12} & ACC_{13} \\ ACC_{21} & ACC_{22} & ACC_{23} \\ ACC_{31} & ACC_{32} & ACC_{33} \end{bmatrix} * \begin{bmatrix} A_X \\ A_Y \\ A_Z \end{bmatrix} + \begin{bmatrix} ACC_{10} \\ ACC_{20} \\ ACC_{30} \end{bmatrix} \tag{2}$$

where: A_{X1} ,A_{Y1} ,A_{Z1} – normalized acceleration along the XYZ axes; A_X , A_Y ,A_Z – unprocessed acceleration along the XYZ axes. Coefficients ACC_{10}, ACC_{20}, ACC_{30} indicate the offset of the accelerometer axes while the remaining ACC coefficients account for non-coaxiality between the axes of the accelerometer and the object of interest as well as for the sensitivity of accelerometer axes.

Calibration of the accelerometer involves determination of twelve coefficients, ACC_{10} through ACC_{33}. We shall consider calibration of the accelerometer in six static positions listed in Table 1. Equation (2) may be written as:

$$\begin{bmatrix} A_{X1} & A_{Y1} & A_{Z1} \end{bmatrix} = \begin{bmatrix} A_X & A_Y & A_Z & 1 \end{bmatrix} * \begin{bmatrix} ACC_{11} & ACC_{21} & ACC_{31} \\ ACC_{12} & ACC_{22} & ACC_{32} \\ ACC_{13} & ACC_{23} & ACC_{33} \\ ACC_{10} & ACC_{20} & ACC_{30} \end{bmatrix} \quad (3)$$

or:

$$Y = W * X \quad (4)$$

where: X – a matrix of twelve calibration coefficients; W – unprocessed accelerometer data (in six positions), Y – matrix of calibrated acceleration values

The calibration algorithm (calculation of coefficients) was divided into two stages, namely the measurement stage and the calculation stage. The measurement stage involves the measurements of accelerations along each of accelerometer axes for all six orientations listed in Table I. The following matrices are afforded:

$$Y = \begin{bmatrix} Y_1 \\ Y_2 \\ Y_3 \\ Y_4 \\ Y_5 \\ Y_6 \end{bmatrix}, \quad W = \begin{bmatrix} W_1 \\ W_2 \\ W_3 \\ W_4 \\ W_5 \\ W_6 \end{bmatrix} \quad (4)$$

TABLE I
UNITS FOR MAGNETIC PROPERTIES

Static positions	AX	AY	Az
Z (up)	0	0	+1 G
Z (down)	0	0	- 1 G
Y (up)	0	+ 1 G	0
Y (down)	0	- 1 G	0
X (up)	+1 G	0	0
X (down)	- 1 G	0	0

The calculation stage involves calculation of calibration coefficients from the following equation (5):

$$X = \left[W^T * W\right]^{-1} * W^T * Y \quad (5)$$

The next stage of calibration procedure consists in calculation of standard deviation σ to eliminate "noise" for each axis in the listed orientations (6):

$$n_{accel} = \frac{1}{N}\sum_{i=0}^{N-1} a_i$$

$$\sigma^2 = \frac{1}{N-1}\sum_{i=0}^{N-1}\left(a_i - n_{accel}\right)^2 \quad (6)$$

Readings smaller than 3*σ are set to zero.

C. Gyroscope calibration

Gyroscope calibration consists in calculation of the offset and standard deviation for every axis. The offset is calculated as a mean value (7):

$$n_{gyro} = \frac{1}{N}\sum_{i=0}^{N-1} g_i \quad (7)$$

The standard deviation is calculated as follows (8):

$$\sigma^2 = \frac{1}{N-1}\sum_{i=0}^{N-1}\left(g_i - n_{gyro}\right)^2 \quad (8)$$

The offset is subtracted from each reading. Gyroscope readings smaller than 3*σ are set to zero. Gyroscope calibration procedure is performed automatically at each device startup.

D. Magnetometer calibration

Measurements of the induction of geomagnetic field are affected by numerous factors. One of these includes hard-iron distortion from magnetized elements within the structure of the device located at near distance from the magnetometer. This interfering magnetic field is added up to the geomagnetic field resulting in an offset of the output signal. Soft-iron distortion is caused by PCB paths or soft magnetic materials. It leads to the vector forming an ellipsoidal shape instead of a spherical shape upon magnetometer rotations. Readout errors are also caused by non-perpendicular orientation of the sensor axes, differences in the sensitivities between individual axes, as well as temperature changes within the system's structure [14].

The relationship between the calibrated magnetometer values M_{x1}, M_{y1}, M_{z1} and unprocessed values obtained directly from the magnetometer M_x, M_y, M_z is as follows (9) [14]:

$$\begin{bmatrix} \mathrm{Mx1} \\ \mathrm{My1} \\ \mathrm{Mz1} \end{bmatrix} = \begin{bmatrix} MR_{11} & MR_{12} & MR_{13} \\ MR_{21} & MR_{22} & MR_{23} \\ MR_{31} & MR_{32} & MR_{33} \end{bmatrix} * \begin{bmatrix} \mathrm{Mx} - MR_{10} \\ \mathrm{My} - MR_{20} \\ \mathrm{Mz} - MR_{30} \end{bmatrix} \quad (9)$$

Coefficients MR_{10}, MR_{20}, MR_{30} represent the offset due to hard-iron distortion while the remaining MR coefficients calibrate soft-iron distortion as well as the errors of sensitivity of magnetometer axes [14]. The goal of the calibration algorithm is to determine the parameters MR_{10} through MR_{33}. To this end, the ellipsoid fitting algorithm developed by Yury Petrov from Northeastern University was used [10].

The goal of the ellipsoid fitting algorithm is to determine the parameters of an ellipsoid matching the cloud of spatial points (magnetic field values M_x, M_y, M_z). As a result of its application, the algorithm delivers the following parameters: the central point of the ellipsoid corresponding to the calibration offsets (MR_{10}, MR_{20}, MR_{30}), ellipsoid radii,

$$\boldsymbol{R} = Ra, Rb, Rc \tag{10}$$

and the matrix of vectors representing the directions of ellipsoid semi-axes:

$$\boldsymbol{Evecs} = \begin{bmatrix} Ra_X & Ra_Y & Ra_Z \\ Rb_X & Rb_Y & Rb_Z \\ Rc_X & Rc_Y & Rc_Z \end{bmatrix} \tag{11}$$

The MR calibration matrix is determined as follows:

$$\begin{bmatrix} MR_{11} & MR_{12} & MR_{13} \\ MR_{21} & MR_{22} & MR_{23} \\ MR_{31} & MR_{32} & MR_{33} \end{bmatrix} = \\ = \begin{bmatrix} Ra_X & Ra_Y & Ra_Z \\ Rb_X & Rb_Y & Rb_Z \\ Rc_X & Rc_Y & Rc_Z \end{bmatrix} * \begin{bmatrix} \frac{1}{Ra} & 0 & 0 \\ 0 & \frac{1}{Rb} & 0 \\ 0 & 0 & \frac{1}{Rc} \end{bmatrix} * \begin{bmatrix} Ra_X & Ra_Y & Ra_Z \\ Rb_X & Rb_Y & Rb_Z \\ Rc_X & Rc_Y & Rc_Z \end{bmatrix}^T \tag{12}$$

Calibration results are presented in Fig. 5.

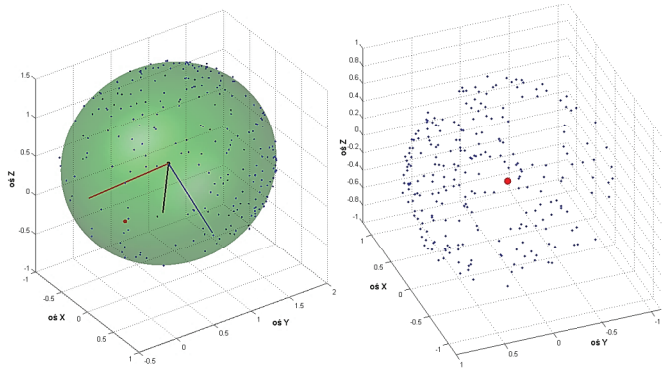

Fig. 5. Results of magnetometer calibration. Unprocessed data with approximated ellipsoid surface (left); after calibration (right).

E. Sensor fusion

Spatial orientation may be determined using the accelerometer, gyroscope, and magnetometer. Although implementation of only one of these sensors is easy, it would be insufficient to deliver appropriate orientation parameters, since each sensor introduces certain errors and limitations. The angular velocity of the gyroscope is burdened by a significant drift, the acceleration measured by the accelerometer is sensitive to noise and fast transient distortions (vibrations) while the magnetometer is sensitive to the magnetic distortions within the variable environment. Therefore, an algorithm is required to perform the fusion of MARG sensor data in order to estimate the object orientation.

This is achieved by implementing the algorithm developed by Sebastian O.H. Madgwick [7]. An advantage of the filter consists in its possibility of being configured using a single β coefficient, very low delays, moderate number of arithmetic operations, ability to operate at low sampling frequencies (starting from 10 Hz) and gyroscopic drift adjustment [7][6][9].

The output of the Madgwick's filter consists in quaternion q representing rotation within a 3D space. This representation allows to avoid the gimbal-lock peculiarity, i.e. a loss of degrees of freedom during the calculations [6]. Example integration results are illustrated in Fig. 6.

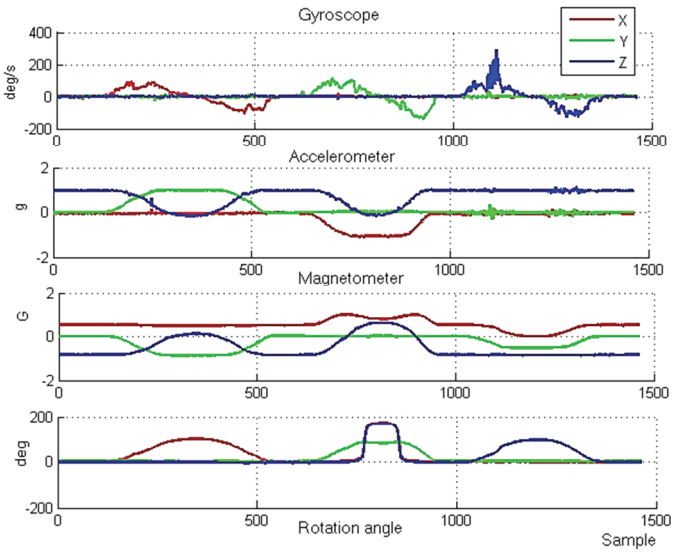

Fig. 6. The result of inertial sensor fusion.

The figure presents the data obtained from the MARG system and the orientation determined using Euler's angles. Rotation around the Y axis is associated with gimbal lock phenomenon manifested as rotations around X and Z axes.

The empirical accuracy of the orientation determination is satisfactory, and therefore the algorithm proves useful in the proposed application area. The accuracy of the measurement is determined by the filter as well as by the parameters of the sensor system. The β coefficient was determined empirically.

IV. Example Applications

Miniaturization of MARG sensors facilitates extension of the area of applications of the manufactured orientation estimation systems. Presented below is the use of the orientation estimation system in the mapping of limb movements.

Fig. 7 presents the method for the capture of upper limb motions. To this end, three orientation measurement systems are placed on the arm, the forearm, and the hand. Knowing the lengths of limb elements and the angles of their spatial orientation, one may produce computer animations and capture the limb motions in real time. Auxiliary axes are plotted on the photograph; locations of the orientation determination systems are marked by arrows.

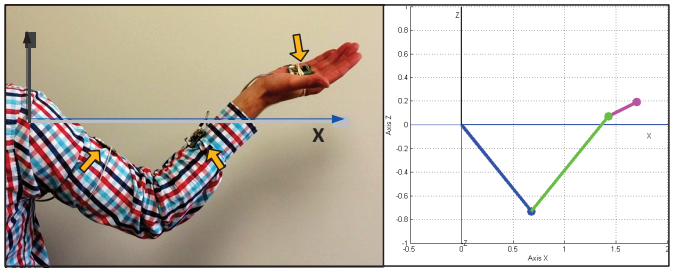

Fig. 7. Capturing the location of the upper limb within the XZ plane.

Modules are connected by power cords and the experimental wired interface. Also presented in Fig. 7. is the view of the desktop script that visualizes the motions recorded by the module. Individual elements between the joints are represented by different-colored segments. Only the XZ plane was presented for better clarity.

In an analogous manner, three measurement systems were placed on the thigh, calf, and foot to capture the motions of the lower limb (Fig. 8).

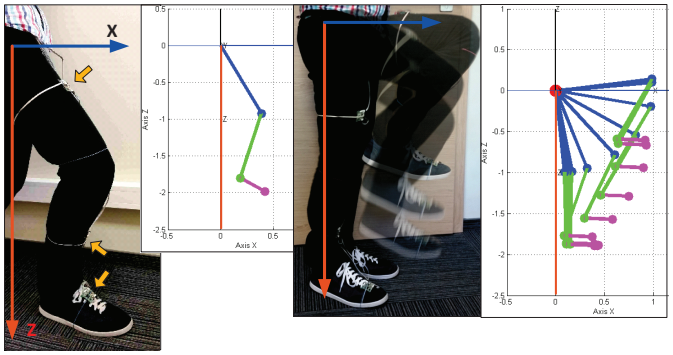

Fig. 8. Capturing the location and motions of the lower limb within the XZ plane.

The systems allow for static capturing of location as well as for the mapping of dynamic changes in positions. Fig. 9 presents the monitoring of the orientation of the foot during ambulation. In order to make the analysis simpler, individual positions of the foot at particular time points were plotted one next to another with constant time offset. Foot orientation is presented as three mutually perpendicular vectors.

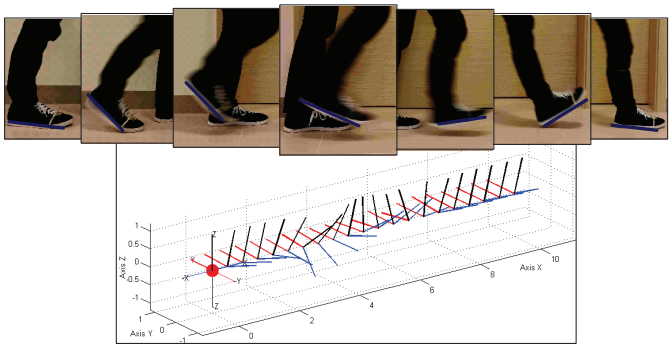

Fig. 9. Capturing the motions of the lower limb.

The errors of the determined orientations of limb segments are due to the design of the sensor and to its flexible fixation causing the device to move in relation to the monitored limb segment during the dynamic tests.

V. Summary

Providing orientation in 3D space using Euler's angles and quaternions increases the flexibility of use of the system according to the above described advantages of both approaches.

Presented hardware solution is characterized by low construction costs, small dimensions, and ease of implementation in all types of systems (especially in wearable electronics systems). The developed measurement system is ready for further studies aimed at achieving better functionality. More stable and functional fixations should be developed to minimize the errors in the estimation of orientation. Detailed studies are required on the accuracy of the estimated orientation in this particular application as well as on the effects of temperature changes on the estimation results. Relevant tests will be performed at a further stage of the project.

References

[1] M. J. Baker, Euler angles, [Online] http://www.euclideanspace.com/maths/geometry/

[2] A. Bronisławski, M. Juchniewicz and R. Piotrowski, "Projekt techniczny I budowa platform latającej typu quadrocopter," *Pomiary Automatyka Robotyka,* no. 1, 2014.

[3] J. Drewniak, "Projekt układu AHRS dla małego quadrotora," Wrocław, Politechnika Wrocławska, 2013.

[4] M. Karbowniczek, "Układy MEMS," *Elektronika Praktyczna,* no.2, pp. 54-56, 2010.

[5] P. Kosiński. P. Świątek-Brzeziński and R.Osypiuk, "Integracja czujników inercyjnych z konstrukcją robota humanoidalnego cz. I," *PAK*, vol. 58, no. 12, 2012.

[6] R. Maciaszczyk, "Porównanie i implementacja metod integracji danych opisanych z wykorzystaniem kwaternionów," PAK, vol. 59, no. 8, 2013.

[7] S. O. H. Madgwick, "An efficient orientation filter for inertial and inertial/magnetic sensor arrays," 2010.

[8] S. O. H. Madgwick, "Quaternions," 2011.

[9] M. Pawełczyk, Raport z realizacji projektu wykonania ramy układu zasilającego, automatycznego systemu sterowania batyskafem i oprogramowania systemu wizyjnego," Gliwice, 2014.

[10] Y. Petrov, Northeastern University, Boston, MA, http://www.mathworks.com/matlabcentral/fileexchange/24693-ellipsoid-fit

Krzysztof Różanowski, PhD. Eng. – Doctor of Philosophy in Technical Science. Alumnus of the Military University of Technology, doctoral degree obtained at the Institute of Biocybernetics and Biomedical Engineering of the Polish Academy of Sciences. Currently the Vice-Director for Research at the Military Institute of Aviation Medicine.
Research scientist conducting studies on optimization of psychophysiological measurements using proprietary microsensor solutions (bioSoc, bioSip) and contactless solutions (EMFi, volumetrically coupled electrodes, microwave sensors, oculographic sensors). Currently engaged, among others, in the development of a specialized BCp (BioChip) technology for acquisition and processing of biomedical signals in the form of submicron CMOS-integrated circuit.
Active participant of conferences on measurement systems and technologies in medicine, author and co-author of 80 Polish and international papers on the subject. Co-author of 16 patent and utility model applications and 30 industrial designs.

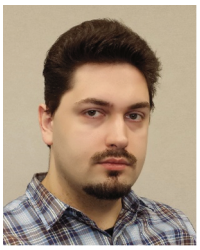

Jarosław Lewandowski, MSc. Eng. – Alumnus of the Faculty of Electronics and Telecommunications of the Military University of Technology. Head of the Medical Electronics Lab and the Head Engineer of the Military Institute of Aviation Medicine. Coordinates the activities of a team of electronic engineers and programmers focusing on the development of human resources and implementation of systems that facilitate the engineering work. A participant in numerous national research and development projects, within both the civilian and military, as well as projects carried out under European programs. Author and co-author of dozens of papers published in Poland or internationally. Scientific accomplishments confirmed by numerous awards and prizes, e.g. the silver medal of Eureka 2010 (Brussels), bronze medal of iENA 2010 (Nuremberg) and gold medal at the IV International Warsaw Invention Show. Co-researcher in the "BioSoC" project awarded the gold medal at the Innova Eureka 2015 fair. Designer of printed circuit boards, low-level software and devices for fabrication of precise mechanical designs.

Marek Placha – Alumnus of the Faculty of Electronics and Telecommunications of the Military University of Technology. A specialist in motion mechanics analysis at the Department of Aviation Bioengineering of the Military Institute of Aviation Medicine. Designer of embedded systems. Currently engaged in the design, research and development of measurement devices in the areas of bioelectronics and bioengineering. Interested in electronics, IT, sports, and cinematography.